Fluidized-Bed Pyrolysis of Polyolefins Wastes: Predictive Defluidization Model

Maria Laura Mastellone and Umberto Arena
Dept. of Environmental Sciences, Second University of Naples, 81100 Caserta, Italy

The risk of defluidization during the low-temperature pyrolytic processes of polyolefins is one of the major constraints to a wider utilization of fluidized beds for the pyrolysis of plastic wastes. A predictive model can estimate the occurrence of defluidization under different operating conditions, taking into account the role of physical properties of the polymers and hydrodynamic variables of the reactor, together with that of the main operating parameters, like the process temperature and the plastic waste feed rate. The results agree well with the experimental data obtained by feeding recycled polypropylene and polyethylene in a laboratory-scale bubbling fluidized-bed pyrolyzer. An operating map allows to distinguish the region of reactor stable operation from that of defluidization.

Introduction

The term "feedstock recycling" indicates a family of advanced technologies for plastic recycling, particularly interesting when the waste has a low grade of homogeneity and is contaminated by nonpolymeric constituents. The polymeric wastes are processed into their basic chemical components that can be used again as raw materials in the production of new petrochemicals and plastics, without any deterioration in their quality and any restriction regarding their application (Kaminsky and Sinn, 1996; Sheirs, 1998).

Fluidized-bed pyrolysis appears as one of the most attractive of feedstock recycling technologies due to: (a) the process flexibility (it can be carried out from 450 to 800°C with different fluidizing gases and plastic mixtures); (b) the possibility to utilize a relatively small scale (making a wider range of investment alternatives); (c) the uniformity of products (due to the very good heat and mass transfer and the consequent and almost constant reactor temperature); (d) the process controllability (increased by the short residence times and the suppression of side reactions as cyclization); and (e) the reduced maintenance time and cost (due to the absence of moving part in the hot regions).

A couple of recent studies (Arena and Mastellone, 2000, 2001), demonstrated that the risk of agglomeration, and of its degeneration until defluidization, must be taken into account in defining design and operating criteria for fluidized-bed pyrolyzers. Actually, agglomeration and defluidization are the more general problems, being present in a number of fluidized-bed processes. Several authors investigated these aspects by using different theoretical approaches (Smith and Nienow, 1983; Seville and Clift, 1984; Compo et al., 1987; Ennis et al., 1991; Seville et al., 1998). The bed defluidization can occur during the pyrolysis of plastics as a consequence of the agglomeration between the molten polymer and the inert material. This phenomenon can occur in different ways, depending on the polymer type, and with different rates, depending on the bed temperature, heat transfer, and other operating conditions as the polymer feed rate and the bed amount. In particular, when recycled polyolefins like polyethylene (PE) or polypropylene (PP) were used in the pyrolysis process, the bed can defluidize as a consequence of sintering between sand particles. These are covered by a layer of polymer that, at a fixed feed rate, could have no time to completely volatilize, thus, becoming progressively larger.

The objective of this work is to develop the theoretical approach proposed in a recent article (Arena and Mastellone, 2001) in order to obtain a model able to predict the set of operating conditions of low temperature pyrolytic processes for plastic waste (Brophy and Hardmann, 1996; Sheirs, 1998) that can lead to defluidization. To this end, the model must take into account hydrodynamic parameters like fluidizing velocity and bed material size, as well as physical properties of the polymer and their variation as a function of temperature.

Predictive Model

The defluidization of the bed during pyrolysis of polyolefins occurs as a consequence of the adhesion between the

Correspondence concerning this article should be addressed to U. Arena.

bed inert particles that are completely covered by a viscous layer of a not yet volatilized polymer. The proposed model aims to predict the time at which this layer becomes large enough that all the inert particles adhere so strongly to each other that the bed sharply defluidizes. The logic of the model includes two successive steps. The first aims to find the time variation of the thickness layer (δ) of the polymer (*thickness growing submodel*); the second one targets to estimate the value for which the layer thickness reaches a value (δ_{crit}) large enough to determine the sintering (*critical thickness submodel*). In the following, the model is described with reference to its application to recycled PP and PE so that the calculated results can be compared with those obtained experimentally in a laboratory-scale fluidized-bed pyrolyzer charged with the same recycled polyolefins (Arena and Mastellone, 2000, 2001).

Thickness growing submodel

A mass balance on the polymer present in the bed at the time t can be written as in the following

$$Q_{Pol} - \mathcal{K}(T)\cdot W_{Pol} = \frac{dW_{Pol}}{dt} \tag{1}$$

where Q_{Pol} is the polymer feed rate, $\mathcal{K}(T)$ is the kinetic constant of the volatilization process (experimentally evaluated for the recycled PP and PE in a parallel investigation by means of thermogravimetric analysis), and W_{Pol} is the amount of polymer present in the bed at the time t. The above-mentioned experiments (Arena and Mastellone, 2000, 2001) indicated that the polyolefins are present inside the bed under the form of layer that covers sand particle surfaces with a thickness δ. Then, it can be written

$$N_s = W_{bed}/\left(4/3\pi r^3\cdot\rho_{sand}\right) \tag{2}$$

where W_{bed} is the bed amount of sand having particle density ρ_{sand}, while r and N_s are the mean radius and the number of sand particles totally covered by the polymer, respectively. Another reasonable hypothesis, that is, the complete mixing of the fluidized bed, imposing allows that N_s coincides with the total number of sand particles of the bed. Therefore, for a plastic polymer having density ρ_{Pol}, W_{Pol} can be written as

$$W_{Pol} = W_{bed}\cdot\frac{\rho_{Pol}(T)}{\rho_{sand}}\cdot\left[\left(1+\frac{\delta(t)}{r}\right)^3-1\right] \tag{3}$$

and it can be substituted in Eq. 1

$$\frac{d}{dt}\left[\left(1+\frac{\delta(t)}{r}\right)^3-1\right]+\mathcal{K}(T)\cdot\left[\left(1+\frac{\delta(t)}{r}\right)^3-1\right] = \frac{Q_{Pol}\cdot\rho_{sand}}{\left(W_{bed}\cdot\rho_{Pol}(T)\right)} \tag{4}$$

The solution of this equation is the expression for the thickness layer at any time under different operating conditions

$$\delta(t) = r\cdot\left[\sqrt[3]{\frac{\dfrac{Q_{Pol}\cdot\rho_{sand}}{W_{bed}\cdot\rho_{Pol}(T)}}{\mathcal{K}(T)}\cdot\left(1-e^{-\mathcal{K}(T)\cdot t}\right)+1}-1\right] \tag{5}$$

In particular, for $t\to\infty$, it gives the expression for the maximum value reachable by the layer thickness δ_∞. It is also possible in this equation to include the polymer density as a function of the temperature. On the basis of the Simha and Boyer theory, Van Krevelen (1972) reported the following relationship

$$\rho_{Pol}(T) = \frac{M}{V_g(298)+\epsilon_g\left(T_g-298\right)+\epsilon_1\left(T-T_g\right)} \tag{6}$$

where M is the molecular weight of the structural unit (equal to 42.1 for polypropylene and 28 for polyethylene). V_g is the molar volume of glassy amorphous polymers (equal to 49.2 for polypropylene, as calculated by adding the contributions for the two groups $-CH_2-$ (15.85), and $-CH-CH_3-$ (33.35) of the polypropylene structure, and equal to 32.9 for polyethylene, calculated in the same way). T_g is the glass transition temperature (253 K for polypropylene and 150 K for polyethylene). ϵ_g and ϵ_l are calculated from the following expressions

$$\epsilon_g = 4.5\cdot10^{-4}V_w$$
$$\epsilon_l = 10\cdot10^{-4}V_w \tag{7}$$

where V_w is tabulated and its value is 30.68 cm^3/mol for polypropylene and 20.46 for polyethylene.

At a temperature of 298 K, the polypropylene density results to be 911 kg/m^3, while that of polyethylene is 873 kg/m^3; at higher temperatures, when the polymers are in the molten state, the variation of the density is negligible.

The Eq. 5 also shows that the thickness growing profile is strongly related to the characteristics of the polyolefin waste and to the main operating variables of the process. In particular, it can be utilized to individualize the different situations that can occur during the polyolefin pyrolysis or, more generally, during the operation of fluidized beds fed with materials that can promote sintering. Figure 1 shows as the polymeric layer thickness grows as a function of time. Two possible situations can occur: (a) the maximum value reached by the layer thickness at steady-state conditions (δ_∞) is lower than the critical one (δ_{crit}), so that there is no risk of defluidization; and (b) δ_∞ is larger than δ_{crit} and defluidization occurs at the time t_{def}, that is when $\delta = \delta_{crit}$. The locus of points for which this condition is satisfied represents the boundary line between the region of stable operation and that of defluidization. A theoretical approach aimed to obtain the value of the critical thickness is reported in the following paragraph.

Critical thickness submodel

This sub-model is based on a force balance on two colliding particles. The balance is written by considering the two particles approaching along the same axis x (Figure 2a). The

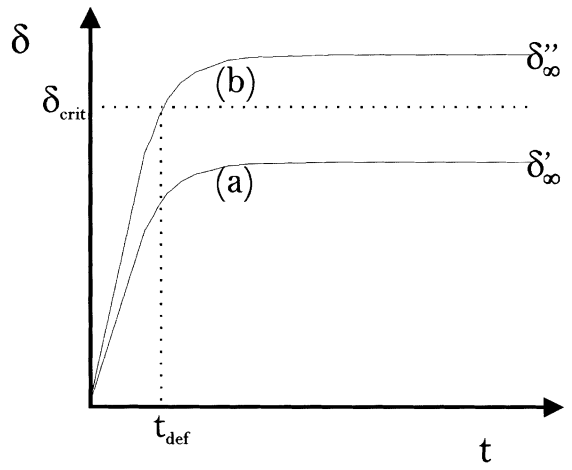

Figure 1. Growth in polymeric layer thickness as obtained by Eq. 5.

(a) Steady value of thickness smaller than the critical one is reached without any risk of defluidization; (b) defluidization condition is reached at time equal to t_{def}.

mean velocity of the two sand particles, having the same diameter and density, and covered by a thickness δ of liquid polymer, is v_o. If the origin of the reference axis is located at the center of one of the two particles (A), the *relative* velocity

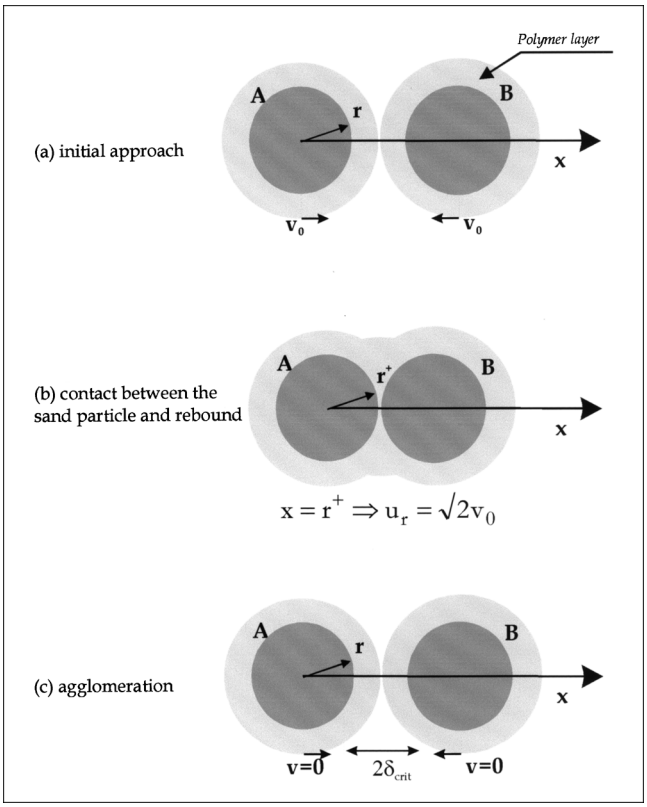

Figure 2. Collision and agglomeration of two particles covered by a critical thickness of polymer layer.

u of the second particle (B) approaching A along the x-axis becomes twice. When the B-surface touches the A-surface, there is a rebound without the separation only if the resistance of the formed liquid bridge overcomes the particle momentum. The resistance is due to the contribution of the capillary and the viscous forces. The capillary contribution to the bridge resistance can be assumed as negligible in comparison with the viscous contribution due to the large value of viscosity. Therefore, the force balance can be, in accordance with Ennis et al. (1991), written as

$$m\frac{du}{dt} = -\pi\mu r^2 u\frac{1}{x} \tag{8}$$

where m is the mass of the particle and μ is the polymer viscosity. The balance leads to the following differential equation: $m\ du = -\pi\mu r^2\ dx/x$ that it has been solved with two boundary conditions at $x = r^+$ and $x = r + \delta_{crit}$. The u values related to these conditions can be derived on the basis of some energetic considerations. Under the assumptions that the collision is perfectly inelastic and the energy loss during the collision and rebound are equal, the following relation is obtained

$$E_{coll} = \frac{1}{2}(E_0 - E_f) \tag{9}$$

where $E_{coll} = 1/2\ mu_{reb}^2$ is the energy of B particle at $x = r^+$, while E_0 and E_f are the energies of the same particle at $x = r + \delta_{crit}$, before the first collision and after the rebound, respectively.

The value u_{reb} of the particle velocity just after the collision and before the rebound has been then obtained by considering (Figure 2b), that the particle energy at $x = r^+$ is half of the difference between the initial energy and the final one. The visualization reported in Figures 2a and 2b indicates that the initial and final energy can be given by

$$E_0 = \frac{1}{2}mu_0^2 = \frac{1}{2}m(2v_0)^2 = 2mv_0^2;$$

$$E_f = 0 \tag{10}$$

as derived by imposing that, at $x = r + \delta_{crit}$, the relative velocity of the B particle is equal to zero. As a consequence, the other boundary condition is: at $x = r^+ \Rightarrow u_r = \sqrt{2}\,v_0$. The following solution of the Eq. 8 is then obtained

$$\delta_{crit} = r\cdot\left[\exp\left(\frac{\sqrt{2}\,mv_0}{\pi r^2\mu}\right) - 1\right] \tag{11}$$

The observed described phenomenology imposes that the mass m has to be written by taking into account the incre-

ment due to the addition of the polymer layer

$$m = m_{\text{sand}} + m_{\text{Pol}} = \frac{4}{3}\pi r^3 \rho_{\text{sand}} + \frac{4}{3}\pi r^3 \left[\left(1+\frac{\delta}{r}\right)^3 - 1\right] \rho_{\text{Pol}}(T) \tag{12}$$

that leads to $m = m_{\text{sand}}$ when $\delta \ll r$.

Equation 11 can be utilized usefully to predict the defluidization time if each operating parameter of the reactor and the intrinsic properties of the polymer are taken into account. In the following, the dependence of v_o on the superficial gas velocity U and that of polymer viscosity on the bed temperature will be detailed.

The particle velocity v_o can be related to the superficial gas velocity in the reactor by means of the relationship reported by Ennis et al. (1991)

$$v_0 = \alpha \cdot \frac{U_B}{D_B} \cdot r \tag{13}$$

where U_B is the rising velocity of a single bubble, D_B is its diameter, r is the bed particle radius, and α is a parameter for which the same authors proposed the value of 12. The bubble rising velocity can be obtained by means of the expression (Allawala and Potter, 1979)

$$U_B = 0.35(gD_{\text{bed}})^{0.5} \tanh^{1/1.8} \cdot \left[3.6\left\{\left(\frac{D_B}{D_{\text{bed}}}\right)^{0.5}\right\}^{1.8}\right] \tag{14}$$

The bubble diameter can be expressed as a function of bed height h by means of the relationship proposed by Darton et al. (1977)

$$D_B = D_B(h) = \frac{0.62(U-U_{mf})^{0.4} \cdot \left[h + 3.37(A_{\text{dis}}/N)^{0.5}\right]^{0.8}}{g^{0.2}} \tag{15}$$

where U_{mf} is the minimum fluidizing velocity, and A_{dis} and N are the area and the number of holes of air distributor plate, respectively.

The value of the particles velocity in the fluidized bed, v_0, as evaluated by Eqs. 13–15, is then a function of the bed height (Figure 3). In order to have a unique value of the critical thickness in the whole bed, a mean value of v_0 is used in the model. It is obtained by averaging v_0 values between $h =$ 0.02m and $h = h_{\max}$, that is, by neglecting the values of v_0 in the first 2 cm above the distributor plate since the bubbles are not completely developed in that area and the validity of the cited equations is not ensured. The maximum height of the expanded fluidized bed $h = h_{\max}$ is, in turn, obtained by evaluating the bed density ρ_{bed} by means of the following equations (Knowlton, 1999)

$$\rho_{\text{bed}} = ABD \cdot (1-\epsilon_B) \tag{16}$$

$$\epsilon_B = (U-U_{mf}) / [U_B + U - U_{mf}] \tag{17}$$

where ABD is the apparent bulk density and ϵ_B is the volume fraction occupied by bubbles. The viscosity of polymers

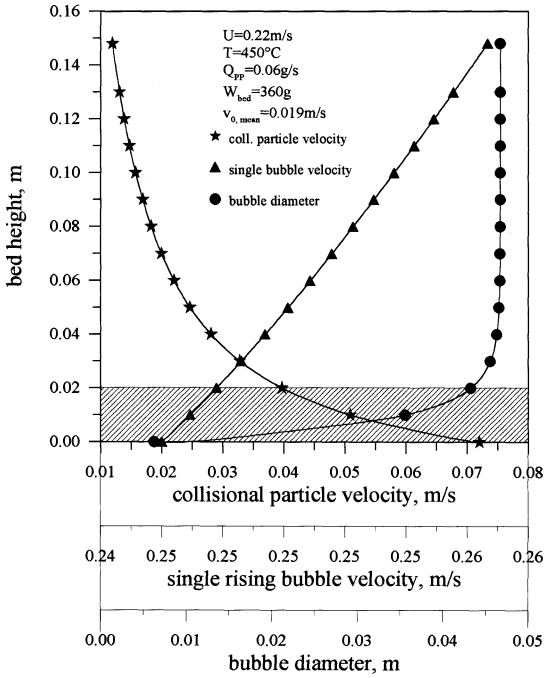

Figure 3. Bed height profiles of the collisional velocity of particles, velocity of the single rising bubble, and diameter of the rising bubble.

in the molten state is a continuous function of the temperature starting from T_g to higher values, well above the melting point. It is related to the critical viscosity μ_{cr} by means of the following expression proposed by Van Krevelen (1972)

$$\log \mu = \log \mu_{cr} + 3.4 \log (M_w/M_{cr}) \tag{18}$$

The critical viscosity can be obtained by means of the relationship

$$\log \mu_{cr} = A(\log \mu^* - B) \tag{19}$$

where A and B are two constants (equal to 2.1 and 1.2 for PP and equal to 1.2 and -0.5 for PE), and where $\log \mu^*$ is graphically obtained as a function of T/Tg (Van Krevelen, 1972).

The critical molecular weight M_{cr} is equal to 8,711 for PP and 3,836 for PE, while the value of the mean molecular weight of each of the two polymers M_w during the pyrolysis process depends on the chain cracking which occurs in the reactor and, therefore, on the main operating variables, like process temperature. A parallel investigation (Incarnato and Acierno, 2000), evaluated that the molecular weight of the tested recycled PP and PE at room temperature are equal to 331,000 and to 235,000, respectively.

Model Implementation and Results

Solving procedure of the model

Figure 4 describes the solving procedure adopted for the proposed model. Two different sets of input data are required: that of hydrodynamics data and that of polymer data.

The symbols in the figure indicate the related variables. The "set of intrinsic data" contains a series of parameters necessary to evaluate intrinsic properties of the polymer by means of the above recalled correlations, like the already defined T_g, V_g, V_w, M_{cr}. Moreover, k_0 and E are the frequency factor and the activation energy of the polymer volatilization rate ($\mathcal{K}$), respectively. Hydrodynamics data provide for the values of some variables, like the minimum fluidizing velocity (evaluated by means of expressions proposed by Geldart (1986)), the bed height, the single bubble rising velocity, and its diameter (Eq. 14 and 15).

As it appears from the graph, the volatilization rate was calculated at the process temperature T that is assumed to be that of the polymeric surface. Note that several experimental observations carried out by means of a scanning electronic microscope (Mastellone and Arena, 1999), showed that

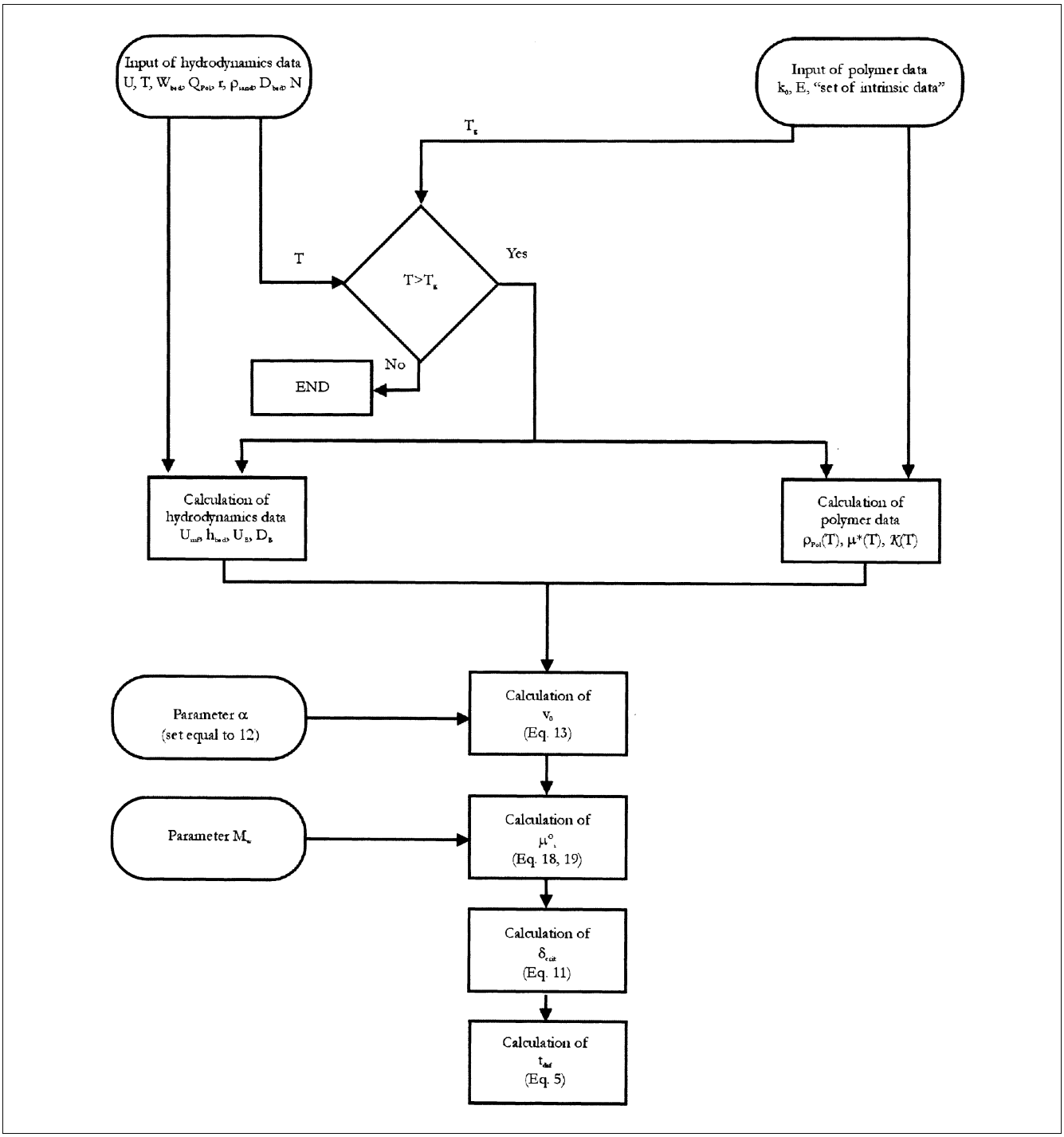

Figure 4. Solving procedure of the model.

the layer covering the sand particle surface has a thickness of about 5–10 μm. This allows a very small value to assume that the whole polymeric layer is at a temperature equal to that of the external surface. This latter assumption has been verified by solving the thermal exchange equations: the results showed that the convective term of the bed is really fast and, in particular, the pellet melts instantaneously (Vettosi, 2001).

The model contains the parameters α and M_w. The first has been assumed to be equal to 12 accordingly with Ennis et al. (1991), even though its value could be lower when the quality of fluidization becomes poor. If the value of α is fixed, it is then possible to obtain the collisional particle velocity profile along the bed height (as reported in Figure 3) and, as a consequence, the mean value of v_0 is utilized in the model computations. It should be noted that neglecting the calculation of the bed height for each operating condition leads to remarkable errors in the value of v_0.

The molecular weight of the degraded polymer that covers the inert material is the actual parameter of the model since its value depends on the polymer type, process temperature,

Table 1. Main Input and Output Data of the Pyrolysis Model of Polypropylene under Typical Set of Operating Conditions (Italic, Output Data)

Hydrodynamic and Process Data	
Reactor temperature, (°C)	450
Feed rate of polymer, Q_{pol} (g/s)	0.06
Bed amount of sand, W_{bed} (g)	360
Superficial gas velocity U (m/s)	0.22
Reactor diameter, D_{bed}, (m)	0.055
Distributor plate holes	100
Voidage of the fluidized bed	0.42
Bulk voidage of stationary bed	0.36
Density of bed material, ρ_{sand}, (kg/m^3)	2600
Bed material mean radius, r_{sand}, (mm)	0.175
Minimum fluidization velocity, U_{mf}, (m/s)	5.32×10^{-2}
Bubble rising velocity (as mean along the bed), U_B, (m/s)	*0.257*
Bubble diameter (as mean along the bed), D_B, (m)	0.0316
α	12
Collisional velocity, v_0 (m/s)	0.0188
Coefficient to verify fluidization regime[a]	0.758
Voidage of expanded bed	0.606
Density of expanded bed, (kg/m^3)	1025
Maximum bed height, (m)	0.148
Polymer Data	
Glass transition temperature, T_g(°C)	−20
Melting temperature, T_f(°C)	183
Degradation temperature, $T_{1/2}$(°C)	387
Molar volume, V_g (cm^3/mol)	49.2
V_w (cm^3/mol)	30.68
ϵ_g	0.0138
ϵ_l	0.0307
Polymer density, ρ_{pol} (kg/m^3)	707
Critical viscosity, μ_{cr} (Pa·s)	9.02×10^{-5}
Generalized viscosity, μ^* (Pa·s)	5.62×10^{-2}
A	2.1
B	1.2
Critical molecular weight, M_{cr}	8711
Θ factor	0.0015
Molecular weight, M_w	95218
Molten viscosity μ(Pa·s)	0.306
Kinetics Data	
Frequency factor, k_0, (s^{-1})	2.22×10^{23}
Activation energy, E, (J/mol)	3.6×10^5
Final output data	
Critical thickness, δ_{crit} (μm)	9.4
Defluidization time, t_{def}, (s)	108

(a) This coefficient is equal to $(D_B/D)^{0.5}$; when its value is >0.38 and <0.7 the bubble diameter is wall affected; when it is >0.7 the fluidization regime is slugging.

Table 2. Experimental and Calculated Defluidization Times for Pyrolysis of PP and PE for Various Values of the Parameter M_w (T = 450°C; U = 0.22m/s; d_{sand} = 350 μm)

Q_{PP} g/s	W_{bed} g	Exp. t_{def}	M_w*[a]	Calc. t_{def} at M_w = 95,218	δ_{crit} μm	Err. %
0.02	240	177	108,500	325	11.2	−84
0.04	240	135	94,500	132	11.2	2
0.06	240	72	97,800	83	11.2	−11
0.073	240	68	95,000	67	11.2	1
0.02	360	384	98,500	472	9.4	−23
0.04	360	166	95,500	174	9.4	−2
0.06	360	135	91,000	108	9.4	17
0.073	360	88	94,500	86	9.4	2
0.04	480	264	90,500	210	8.2	20
0.06	480	155	90,800	128	8.2	17
0.073	480	126	90,800	102	8.2	19
Q_{PE}, g/s	W_{bed}, g	Exp. t_{def}	M_w*[a]	Calc. t_{def} at M_w = 7,815	δ_{crit} μm	Err. %
0.02	240	312	8,000	355	12.3	−14
0.04	240	135	7,900	142	12.3	−5
0.06	240	94	7,700	89	12.3	5
0.073	240	81	7,600	72	12.3	11
0.02	360	333	8,450	527	10	−58
0.04	360	150	8,200	187	10	−25
0.06	360	127	7,650	115	10	9
0.073	360	111	7,450	92	10	17
0.04	480	190	8,120	226	9	−19
0.06	480	157	7,550	137	9	13
0.073	480	141	7,350	109	9	23

[a]Mw^* is the value of the parameter M_w which perfectly fits modeling and experimental results.

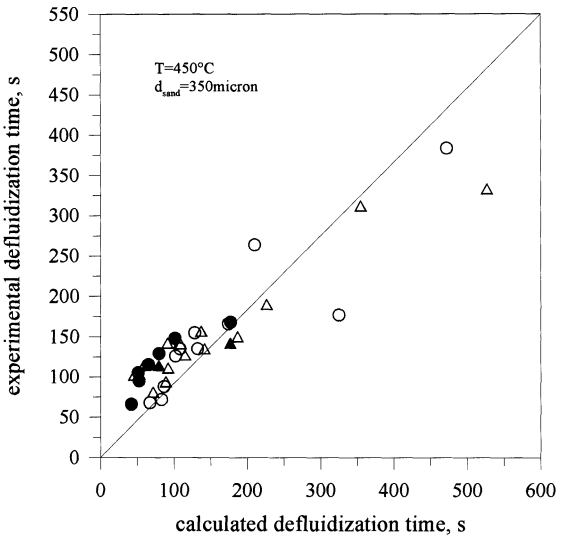

Figure 5. Experimental vs. calculated defluidization times for tests with PP (circle) and PE (triangle).

Open symbols refer to tests at U = 0.22m/s; shaded symbols refer to tests at U = 0.4 m/s.

The molecular weight of the degraded polymer that covers the inert material is the actual parameter of the model since its value depends on the polymer type, process temperature,

heating rates, and reactants used. For the tested polymers, the initial value of the molecular weight could theoretically decrease until 0 during the thermal process. The value of M_w utilized in the model for each polymer has then been obtained as a mean of the values, which perfectly fit modeling and experimental defluidization times. Once the molecular weight is fixed, the model provides for the defluidization time by imposing $\delta(t_{def}) = \delta_{crit}$ and by adequately arranging the Eq. 5.

Comparison between experimental and modelling results

The main input data of the model are listed in Table 1 together with the related output data for a typical set of operating conditions.

The variation of defluidization times for operations with PP and PE is exemplified in Table 2 for a typical set of conditions (bed temperature = 450°C; fluidizing velocity = 0.22 m/s; Sauter mean diameter of bed material = 350 μm), and under different values of plastic waste feed rate and bed holdup. The table also includes experimental defluidization times measured during the tests carried out under the same operating conditions in a bubbling fluidized-bed reactor, 55 mm ID (Arena and Mastellone, 2000, 2001). The good agreement between experimental and modeling results is further highlighted for both the plastic wastes tested by data in Figure 5. There is a remarkable disagreement for only two situations, both related to the small scale of the experimental reactor, which affected the measured t_{def}: the inaccurate performance of the mechanical feeder, sometimes observed at the lowest value of polymer feed rate (0.02g/s) and the bed slugging regime, which established at the highest value of fluidizing velocity.

Note that Table 2 also reports calculated values of δ_{crit}: all of them are in the range experimentally measured by means of SEM observations.

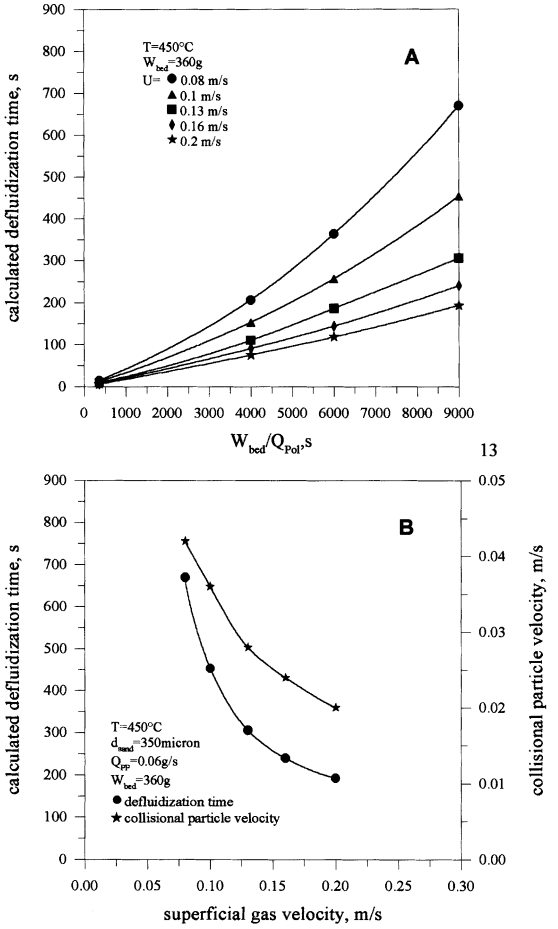

Figure 7. Calculated defluidization times for PP pyrolysis as a function of the ratio between bed amount and polymer feed rate (A) and as a function of the fluidizing velocity (B).

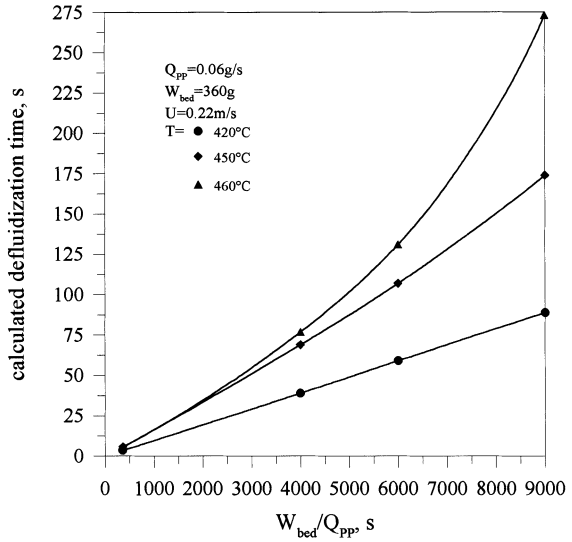

Figure 6. Calculated defluidization times for PP pyrolysis as a function of the ratio between bed amount and polymer feed rate and for different reactor temperatures.

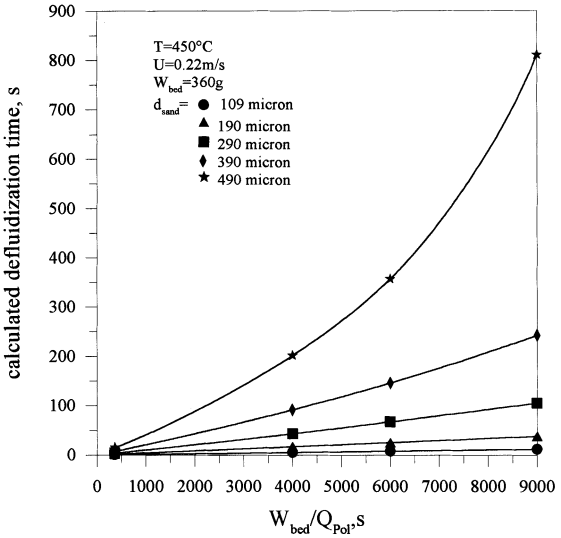

Figure 8. Calculated defluidization times for PP pyrolysis as a function of the ratio between bed amount and polymer feed rate and for different mean diameters of the inert particles.

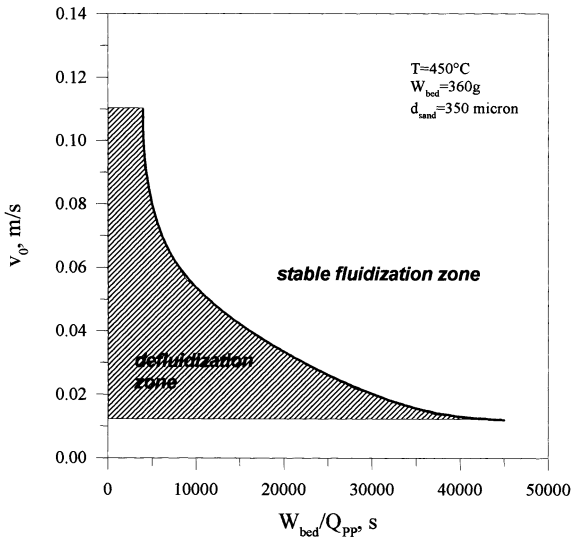

Figure 9. Operating map of PP pyrolysis at 450°C, showing the zone of stable fluidization and defluidization.

Effect of operating parameters on the defluidization time

The experimental studies on the phenomenology of bed defluidization that have often been recalled, above clearly showed the crucial role of the ratio between the holdup of inert material and the polymer feed rate. For this reason, the following analysis of the influence of other operating parameters on the defluidization time has been related to this key variable. The diagrams in the following refer always to PP, due to the absolutely coincidental behavior of PE.

Figure 6 reports the variation of t_{def} as a function of W_{bed}/Q_{Pol}, for different values of the parameter reactor temperature. As expected, the bed temperature has a crucial effect on the defluidization behavior of the bed: a limited increase can delay or completely avoid the risk of defluidization since the temperature strongly affects the volatilization rate, as well as the molten polymer viscosity. The model also predicts when the temperature is sufficiently high to avoid any risk of defluidization: for instance, at 500°C, the model indicates no defluidization, as experimentally verified in a run as long as 5,400 s.

The effect of the fluidizing gas velocity is described by Figures 7a and 7b, where the calculated defluidization time is reported as a function of W_{bed}/Q_{Pol} for a five series of runs (Figure 7a), and as a function of the superficial gas velocity, together with the collision particle velocity, for a specific set of operating conditions (Figure 7b). An increase of U results in a decrease of v_0 and, then, to a faster defluidization of the bed. For instance, t_{def} reduces more than 50% when U increases from 0.1 to 0.2 m/s. This finding clearly indicates that the increase of fluidizing velocity is not a correct operating criterion to avoid the bed sintering.

A longer defluidization time could be obtained instead by using coarser particles as bed material. This effect is described in Figure 8 and it is related to the larger collisional particle velocity.

An operating map for defluidization is finally presented. As mentioned above, the locus of points for which $\delta_\infty = \delta_{crit}$ represents the boundary curve between the region of stable operation and that where defluidization occurs. The relationships for δ_∞ and δ_{crit}, that is, Eqs. 5 and 11, suggest that, for a fixed reactor geometry, for a fixed polymer, and at a fixed-bed temperature, these values of layer thickness depend only on the ratio W_{bed}/Q_{Pol} and on the collisional velocity v_0. This leads, for a bed temperature of 450°C, to the curve in Figure 9, valid in the range of admissible values of v_0 for the reactor geometry used in the test, that is, $v_0 > 0.012$ m/s (means U less than the threshold gas velocity for turbulent regime), and $v_0 < 0.11$ m/s (means U greater than minimum fluidization velocity). The agreement with the experimental evidence is complete. At 450°C, all the observed defluidization tests fall in the lower region of the map, that is, below the limit condition for a stable operation. At 500°C, the three experimental conditions tested never showed defluidization as predicted by the position of the related points on the operating map.

Table 3. Sensitivity of the model to parameters α, M_w, and U

Q_{PP} g/s	W_{beb} g	d_{sand} μm	U m/s	α	M_W	Calc. t_{def}	S
0,06	360	350	0.22	8		68	
				12	95,218	108	1.05
				10		87	
0,06	360	350	0.22	12	85,218	171	
					95,218	108	−4.32
					105,218	73	
0,06	360	350	0.1 (v_0 = 0.036 m/s)	12	95,218	245	
			0.22			108	−1.23
			0.4 (v_0 = 0.012 m/s)			65	

The sensitivity of the model to the variation of the parameter M_w has been carried out with the standard procedure for linearized sensitivity (Rudd and Watson, 1968). The same analysis has been also developed for the α parameter and the fluidizing gas velocity U. Each parameter was changed by a fraction of its allowable range of variation. For α, on the basis of values listed in Table 2, it has been considered a variation -2 and -4; for M_w, a variation of $\pm 10{,}000$, U has been varied between 0.1 and 0.4 m/s. The sensitivity of the output variable t_{def} was evaluated as: $S = [(t_{def}^- - t_{def}^+)/t_{def,b}]/[(v^- - v^+)/v_b]$ where subscript b indicates the base case value. Superscripts $-$ and $+$ indicate, for the generic input variable v, the left and right extremes of the assumed range of variation, whereas, for the output variable t_{def}, they indicate the values that it assumes for these extremes. The results shown in Table 3 indicate that the model has a high sensitivity to the molecular weight, which results to be the true parameter of the model.

Conclusions

A mathematical model able to predict the occurrence of defluidization during the fluidized-bed pyrolysis of polyolefins has been developed. The model takes into account the operating variables of the process and the intrinsic properties of the polymers.

The computed values of defluidization times are in good agreement with those experimentally measured in a laboratory-scale bubbling fluidized-bed pyrolyzer continuously operated with recycled polypropylene and polyethylene.

The effect of the main operating variables has been investigated and an operating map able to define the region of reactor stable operation and that of bed defluidization is eventually presented.

Acknowledgments

The study has been carried out with the financial support of the Italian Minister for University and Scientific Research (PRIN Projects). The authors are indebted with Giulio Vettosi for his helping in performing model calculations.

Literature Cited

Allawala, J., and O. E. Potter, "Rise Velocity Equation for Isolated Bubbles and for Isolated Slugs in Fluidized Beds," *Ind. Eng. Chem. Fund.*, **18**, 112 (1979).

Arena, U., and M. L. Mastellone, "Defluidization Phenomena During the Pyrolysis of Two Plastic Wastes," *Chem. Eng. Sci.*, **55**, 2849 (2000).

Arena, U., and M.L. Mastellone, "The Phenomenology of Bed Defluidization during the Pyrolysis of a Food-Packaging Plastic Waste," *Powder Tech.*, **120**, 127 (2001).

Brophy, J. H., and S. Hardman, *Recycling and Recovery of Plastics*, J. Brandrup et al., eds., Hanser Publishers, New York, pp. 435—444 (1996).

Compo, P., R. Pfeffer, and G. Tardos, "Minimum Sintering Temperatures and Defluidization Characteristics of Fluidizable Particles," *Powder Tech*, **51**, 85 (1987).

Darton, R., R. La Nauze, F. Davidson, D. Harrison, "Bubble Growth due to Coalescence in Fluidised Beds," *Trans. Instn. Chem. Engrs.*, **55**, 274 (1977).

Ennis, B. J., G. Tardos and R. Pfeffer, "A Microlevel-Based Characterization of Granulation Phenomena," *Powder Tech*, **65**, 257 (1991).

Geldart, D., *Gas Fluidization Technology*, Wiley, New York (1986).

Incarnato, L. and D. Acierno, private communication, University of Salerno, Italy (2000).

Kaminsky, W., and H. Sinn, *Recycling and Recovery of Plastics*, J. Brandrup et al., eds., Hanser Publishers, New York, pp. 435–444 (1996).

Knowlton, T., PSRI Fluidization XXXV Seminar and Workshop, Chicago (Oct. 5–8, 1999).

Mastellone, M. L. and U. Arena, "Carbon Attrition during the Circulating Fluidized Bed Combustion of a Packaging-Derived Fuel," *Combustion and Flame*, **117**, 562 (1999).

Rudd, D. F., and C. C. Watson, *Strategy of Process Engineering*, Wiley, New York (1968).

Seville, J. and R. Clift, "The Effect of Thin Liquid Layers on Fluidisation Characteristics," *Powder Tech*, **37**, 117 (1984).

Seville, J., H. Silomon-Pflug, and P. Knight, "Modelling of Sintering in High Temperature Gas Fluidization," *Powder Tech*, **97**, 160 (1998).

Sheirs, J., *Polymer Recycling*, Wiley, New York (1998).

Smith, P. G. and A. W. Nienow, "Particle Growth Mechanisms in Fluidised Bed Granulation-I. The Effect of Process Variables," *Chem. Eng. Sci.*, **38**, 1223 (1983).

Van Krevelen, D. W., *Properties of Polymers: Correlation with Chemical Structure*, Elsevier, Amsterdam (1972).

Vettosi, G., "Fluidized Bed Pyrolysis of Polyolefins," Chemical Engineering Bachelor's Degree Thesis, University "Federico II" of Naples (2001).

Manuscript received June 20, 2001, and revision received Jan. 2, 2002.